

GeoArch

Report 2011/41

Archaeometallurgical residues from
field D5, near Porthworthy, Shaugh
Prior, Devon (Avon SWW Pipeline)

Archaeometallurgical residues from field D5, near Porthworthy, Shaugh Prior, Devon (Avon SWW Pipeline)

Dr T.P. Young

Abstract

Five pieces of slag from cut feature [1154] in field D5 (near Porthworthy, Shaugh Prior, Devon) of the Avon SWW pipeline were examined and determined to be residues from iron smelting. The field record of the location of the residues is consistent with the interpretation of the feature as the basal pit of a non-slag tapping 'slagpit'-style iron smelting furnace, with the slag left in-situ in the pit after its last use. Such furnaces were the characteristic style of smelting furnace in the pre-Roman Iron Age and were used again in the early medieval period between the 5th and 9th centuries.

The slag samples showed closely related bulk elemental composition and mineralogy. The similarity was sufficient to be compatible with the origin of all the materials during a single smelt, or within different smelts undertaken with a similar process and materials. The only element not forming a fairly simple trend was manganese, and this is known to be very unevenly distributed in many iron ore bodies and also possibly to be unevenly concentrated within the slags of a single smelt.

Identification of the ore type that was smelted is uncertain. The key characteristic of the ore is that it appears to have been a fairly pure iron ore with an appreciable (perhaps up to 2% quoted as an oxide) manganese content, but with low phosphorus and calcium contents. Local gossan iron ores occur near Shaugh Prior (the Dewerstone Iron Mine) and ores of this type are a possible source, but historic analysis indicates only a trace manganese content at this mine. An alternative origin for a relatively manganiferous ore would be a bog iron ore, but most bog iron ores contain higher concentrations of calcium and phosphorus than recorded here. The silica to alumina ratio for the slags is extremely low (average 2.6) resulting in a very high alumina content in the slags of 7-11 wt%. Such levels, and the resultant hercynite-rich mineralogy, are relatively unusual in pre-medieval slags. High alumina ore and high manganese/low phosphorus ores were found at Kestor, but none is currently known in SW Devon. Although the high alumina levels may be due to the iron ore, it is also possible that this was a result of local kaolinic clays being used for furnace construction.

Contents

Abstract	1	Glossary	5
Methods	1	References	7
Results		Figure Captions	8
Description of the Samples		Table 1. Material sampled from D5	9
AVN21	2	Table 2: Area EDS analyses of typical areas	10
AVN22	2	Table 3. EDS analyses of phases	11
AVN23	3	Table 4. comparative analyses	16
AVN24	3		
Distribution of the residues	3		
Interpretation	4		
Discussion	4		

Methods

Materials from this site were assessed together with those from site D1 (Young & Kearns 2011). The assessment recommended further investigation because the field identification of the materials as tin slags was suspect.

From the materials examined for the evaluation, a variety of samples were selected as being possibly suitable for analysis and four samples (Table 1) were taken forward for detailed analysis.

Electron microscopy was undertaken on the Cambridge Instruments (LEO) S360 analytical electron microscope in the School of Earth and Ocean Sciences, Cardiff University. Microanalysis was undertaken using the system's Oxford Instruments INCA ENERGY energy-dispersive x-ray analysis system (EDX). All petrographic images presented in this report are backscattered electron photomicrographs. The polished blocks for investigation on the SEM were prepared in the Earth Science Department, The Open University.

Throughout this report standard mineral terminology is applied to both natural and anthropogenic materials – although artificial phases are no longer strictly considered to be minerals.

The convention adopted in this report is to describe olivine bearing Fe, Mg, Ca and Mn in terms of an olivine on the forsterite-fayalite join (using the notation for instance of Fa95Fo5 for an olivine that is 95% fayalite and 5% forsterite; where $Fe/(Fe+Mg) = 0.95$) plus figures for the overall percentage replacement by calcium and manganese.

This report was undertaken for Historic Environment Projects, Cornwall Council.

Results

Description of the samples

AVN21

Sample AVN21 included two separate slag blebs within a single mount:

Particle A (Plates A1-A2) – this bleb was moderately, but finely vesicular. The slag was of a very heterogeneous texture, with blebs rich in wustite, 500-800 μm across, in a more general slag composition with primary wustite in moderately stout dendrites with arrays of up to 200 μm , followed by elongate fayalite of up to 500 μm length and 50 μm width. The interstitial areas are often very poorly preserved, but locally survive and show small grains and more elaborate stout dendrites of hercynite typically nucleated either on exposed wustite or within the outermost layers of the fayalite, followed by a glass bearing fine crystals, possibly also of olivine.

EDS analysis shows the wustite-rich patches with an iron content of 84% FeO, 10% silica and 4% alumina, whereas the more typical texture was 63-68% FeO, 20-22% silica and 7-10% alumina. Manganese contents were moderately high at 1.6-2.0% MnO. The levels of magnesium, calcium, sodium and potassium were all low. Phosphorus was below detection in the analysed areas.

The analysed fayalite showed a composition of Fa96Fo4 in crystal cores to Fa100 (end-member fayalite) with about 4% of manganese substitution. Calcium substitution was low, typically less than 1%, rising to 3% on some margins and possibly higher in the interstitial olivine (although analysis of the interstitial olivines is unreliable because of their small size).

The hercynite contained between 10 and 15% magnetite, with 2-4% manganese substitution and up to 1% titanium substitution.

The interstitial glass was aluminous with 20-23% alumina and 39-40% silica. The glass contained approximately 0.7% P_2O_5 , 0.3% S, 3.0-3.6% Na_2O , 9-10% K_2O and 5% CaO .

Particle B (Plate A3) – this bleb was more homogeneous and coarser grained than particle A. There was very sparse development of a primary wustite, forming poorly developed dendrites of up to 300 μm across, but usually much less.

The dominant mineral was olivine, which formed complex crystals at least 600-800 μm in length and 100 μm in width. The inner parts of each olivine crystal formed a syntectic with wustite and the outer parts formed a coarse syntectic with hercynite.

The interstitial areas were again poorly preserved, but were typically rich in leucite – either on its own or in a syntectic structure with wustite.

The bulk composition was lower in iron than particle A, with 61-66% FeO, 23-26% silica and 7-8% alumina. Manganese was rather more abundant than in particle A, with approximately 2% MnO. Levels of calcium and magnesium were again low (less than 1% of each oxide). Sodium was more abundant than in particle A (at 1.0-1.2% Na_2O), but potassium appeared rather low (0.6-0.7%) despite the relative abundance of leucite.

The olivines ranged from Fa96Fo4 with 4% manganese substitution (in the syntectic with wustite) to Fa100 with 3% manganese substitution and up to 3% calcium substitution (in the syntectic with hercynite). The elevated levels of manganese substitution are in keeping with the elevated bulk manganese concentration.

The hercynite composition was similar to that in particle A, with 11-13% magnetite and 3% manganese substitution and 2% titanium substitution.

AVN22 (Plate A4)

This sample was a moderately vesicular slag, with a heterogeneous microstructure, incorporating wustite-rich patches (e.g. Plate A4e) and some areas of coarse olivine with relatively little wustite (e.g. Plate A4c, left of centre), set in a more typical slag (Plate A4c, right of centre) comprising abundant coarse primary wustite dendrites (ranging from delicate arrays of up to 500 μm , down to much smaller, stout arrays with curvilinear components) followed by elongate olivine of up to 600 μm by 100 μm .

As with the other specimens, the interstitial areas are heavily corroded. The outer parts of the olivine crystals commonly show a syntectic relationship with hercynite (which also occurs as stubby dendrites in the interstitial areas). There are commonly small hercynite crystals

which also occur intergrown in the outer layers of the wustite (Plate A4 b and d).

The bulk composition of this sample is markedly more iron rich than the other samples, with 71-75% FeO in the typical texture and up to 86% FeO within the wustite-rich blebs. The sample has correspondingly low levels of silica and alumina (15-18% and 5-7% in the typical texture respectively), and low levels of magnesium, calcium, sodium and potassium. In contrast, manganese is moderately elevated at 1.7-2.0% MnO in the typical texture.

The olivine shows compositions of Fa97Fo3 to Fa100 (from core to margin) with about 4% Mn substitution. Hercynite compositions appeared comparable with those in the other samples, but corrosion of the interstitial spaces meant that these analyses were not reliable.

AVN23 (Plate A5)

This sample again showed a rather heterogeneous texture. There is a low proportion of large, but sparse, wustite dendrites of up to 600 µm across. The dominant component of the texture is formed by clumps of large olivine crystals. The individual complex crystals appear to be at least 1mm in length and 300 µm in width. The clumps of crystals are up to at least 2mm across and show a crude radial structure.

In some clumps, the olivine is cored with a wustite-olivine syntectic and the outer parts of the crystals are a hercynite-fayalite syntectic, but in other are the olivine is almost entirely in a syntectic with hercynite.

The areas which are interstitial to the main olivine clumps are mainly themselves dominated by a second generation of small olivine crystals (up to a maximum size of 200 x 30 µm), with a third generation of fine dendrites, probably also an olivine, in the interstitial glass (Plate A5 b, f, g). Some rarer, small, interstitial areas contain a leucite-wustite syntectic (Plate A5 d, e).

This slag was the least iron-rich of the samples with only 56-61% FeO. All other elements were correspondingly elevated (with silica of 26-27%, alumina 9-10%, magnesia 0.4-0.8%, lime, 0.8-1.4%, soda 0.6-0.8% and potash around 2% in typical areas).

The olivine varies from Fa95Fo3 to Fa97Fo3 with the inner parts of the olivine, all with about 4% manganese substitution. In the olivine with the syntectic relationship to hercynite, the composition varies from Fa97Fo3 to Fa100 with 4% manganese substitution and commonly 1% calcium substitution.

The hercynite is similar to that of the other samples, with 10-15% magnetite and with 2-3% manganese substitution and 1% titanium substitution.

One area showed the rare occurrence of a layered structure including a rare earth element-bearing calcium phosphate, intergrown with an unidentified iron-bearing mineral.

AVN24 (plate A6)

This material was strongly heterogeneous, varying from a rather granular, vesicular texture at one end, through a central section rich in charcoal to a finely quench-textured chilled lobe at the other end.

The quench textured zone shows very delicate primary wustite dendrites of up to 100 µm across, followed by sheaves of olivine in crystals of up to 1mm in length but only 20 µm in width. These appear to have nucleated on the well defined chilled margin of the piece.

The charcoal-rich zone contains mineralised charcoal clasts of up to a few millimetres across. Between this clasts are some rounded lobes of slag (Plate A6 h) with textures rather similar to, but somewhat finer than, that of AVN21 particle B.

The more granular areas show rather equant subhedral olivine crystals generally of up to 200 µm across, which enclose rounded grains of wustite (which although frequently aligned do not appear to constitute dendritic elements) and angular, euhedral grains of hercynite (themselves sometimes enclosing wustite).

This granular zone is highly vesicular (vesicles of up to at least 600 µm). The vesicles are commonly bounded by complex zones of leucite and leucite-wustite syntectic. These materials tend to occupy much of the interstitial space away from the major vesicles too – and in some areas seem to form large vesicular patches (Plate 6a, lower margin).

The bulk composition of the slag in this sample was typically rather iron-poor (56-65% FeO). The slag was rich in silica (19-26%), alumina (8-11%), manganese (4-5%), lime (1.0-1.6%) and potash (0.2 to 1.6%) compared with many of the other samples.

Analysed olivine varied from Fa95Fo5 with 1% of calcium and 10% of manganese substitution to Fa98Fo2 with 3% calcium and 9% manganese substitution. The hercynite was 10-14% magnetite with 5-6% manganese substitution and 1-3% titanium substitution.

Distribution of the residues

The supplied plan and section of feature [1154] show an elliptical cut 0.48m by 0.36m and 0.18m deep. The photograph and section show slag block (1429) overlying approximately 0.15m of slag-rich fill (1186). The slag block rests against the NW side of the furnace pit, and the opposing wall shows a variety of fills, interpreted as an earlier pit filling truncated by a redig, but other interpretations are possible.

The presence of a major slag block (the so-called 'furnace bottom', FB, of Crew 1985, 1986) against one side of the pit of a slagpit furnace and not extending across its full width is a typical features of both Iron Age (e.g. Young 2003a, 2003b, 2005, 2006) and early medieval furnaces (e.g. Haslam 1980; Reed *et al.* 2006; Young 2011b).

The sample AVN24 derives from (1429) and is compatible with an origin within a FB. The smaller slag pieces (AVN21, AVN22 and AVN23) will represent slag drips that have descended into the pit below the FB.

The photographs show the reddening of the pit margins at the level of truncation, but there is insufficient detail to observe any variation in the oxidised zone. The most likely interpretation would be that the furnace was blown from the NW, where the FB is in contact with the pit margin.

Interpretation

The five pieces of analysed slag showed closely-related chemical compositions and mineralogies. Since the concentrations of other elements are low, the samples can reasonably be displayed on a $\text{SiO}_2\text{-Al}_2\text{O}_3\text{-FeO}$ ternary diagram (Figure 1). These show the bulk analyses of the samples forming a linear array trending away from the FeO pole. This pattern would be that expected for a smelting system, if the samples were either from a single smelt, or from closely related smelts.

The trend of the array is between the FeO pole and a point at about $\text{SiO}_2 = 74\%$, $\text{Al}_2\text{O}_3 = 26\%$ (i.e. $\text{SiO}_2:\text{Al}_2\text{O}_3 = 2.8$). A simple numerical average of the $\text{SiO}_2:\text{Al}_2\text{O}_3$ ratio in the analysed areas is approximately 2.6, being influenced by a scatter of some points from AVN22 and AVN24 which lie off the main trend. This low silica to alumina ratio is a product of a high concentration of alumina in the samples (7-11 wt%), and is reflected in the abundance of hercynite in the samples.

Hercynite-rich slags were considered by Morton & Wingrove (1969, 1972) to be characteristic of medieval iron smelting slags rather than earlier examples. They associated the more aluminous slags with the onset of smelting of claystone ores from the Carboniferous coalfields in the medieval period. Spinel-rich slags characterise the most extreme examples of such materials) and these may be associated with high levels of iron extraction from the claystone ores after the introduction of water-powered bloomeries in around the 14th-15th centuries (e.g. Dungworth 2010). Slightly earlier hercynite-rich slags were described by Young (2011) from both a 14th-15th century water-powered site and a 13th century manually-blown bloomery in Shropshire. The perceived problem for early smelters with the more aluminous systems is that the liquidus temperature rises rapidly in the hercynite field (Figure 1). In this instance, however, the analyses are close to the hercynite-fayalite divide and the liquidus temperatures involved were probably close to or below 1200C.

The origin of the high alumina content of the slag might be from a high alumina ore, but might also be due to incorporation of high alumina ceramic from the furnace. During the smelting of a high grade iron ore it will be the furnace lining that is the major contributor to the alumina and silica of the resultant slag (Thomas & Young 1999a and 1999b).

Besides the high alumina content, some of the key features of the slag composition are the high manganese content and the low concentrations of phosphorus and calcium. These properties, together with the known geological context in SW Devon, suggest three possible origins for the ore:

1. a bog iron ore – these typically show elevated manganese contents, but also tend to show moderate calcium and often moderate to high phosphorus contents. Examples of such ores and the slags generated from their smelting are now known widely in Ireland (e.g. Young 2011b), but there are also examples known from Wales (e.g. Crew 1987, 1989, 1998), Shropshire and the Thames Valley (e.g. Young 2005).
2. a gossan ore – these occur widely in the SW England Orefield, with the closest documented example at Shaugh Prior (Dines 1956, p.686). A historic analysis of ore from Shaugh Prior was quoted by Dines (1956, p. 686; Table 4). This analysis shows

a high grade iron ore, with only a trace of manganese, but with high phosphorus (1.85% P_2O_5). The chemistry of other SW England gossans has not been explored much using modern methods, but the Truro College site (Young 2008) produced both gossan ores and corresponding smelting slags. They showed elevated manganese (up to 1.35% MnO in the ore, up to 3.4% in the slags), but much once again much more elevated phosphorus than the present material (up to 1.07% P_2O_5 in the ore and 1.0% in the slags). In addition, the Truro gossans showed a high silica: alumina ratio, unlike the present material. However, despite this, the smelting slags showed a similar mineralogy to the present examples – with a fayalite-hercynite syntectite forming the outer parts of the fayalite crystals in the flow slag samples.

3. other vein hematite ore – these are not well known, but are common in some areas, for instance the NE of Dartmoor. Material from Kestor currently held by Peter Crew has been analysed and shows, apparently, two hematite ores, one of which is mixed with kaolinite and the other with a high manganese content (1.43% MnO). Both the Kestor ores have extremely low phosphorus contents.

Thus interpretation of the ore smelted on the present site cannot be interpreted with ease. The low phosphorus content and high manganese content does not resemble what little is known of the nearby gossan ores at Shaugh Prior, although a high manganese content was observed in gossan ores from Truro. What is known of both of the gossan ores shows a high phosphorus content, however. High manganese, low phosphorus and possibly a low silica:alumina ratio are features matched by a hematite ore from Kestor, but similar ores have not, to the author's knowledge, been recorded from SW Dartmoor. A high manganese content may be a feature of bog iron ores and not all of these have strongly elevated phosphorus contents (although many do), but most show slightly elevated levels of calcium.

On balance, a minor occurrence of vein iron ore similar to those of NE Dartmoor is probably the most likely source.

Discussion

The evidence clearly indicates that [1154] was the pit below a non-slag tapping 'slagpit' furnace. Such furnaces were the principal form of iron smelting furnace in the pre-Roman Iron Age, but became replaced by a variety of slag-tapping furnaces during the Roman period. After the Roman period the slagpit furnace returned, but was again replaced by slag tapping furnaces, probably in about the 9th century (as part of a general technological change which spread across most of northern and northwestern Europe, except Ireland; Pleiner 2000).

In the SW, slagpit furnaces have been recorded at Truro (Young 2008), Berry Ball (Young 2009) and Trevelgue Head (Dungworth 2011) in the Iron Age and at Burlescombe (Reed *et al.* 2006) and possibly Kestor (Fox 1954) from the early medieval period.

Many of the occurrences of slagpit furnaces are those structures which used to be termed bowl furnaces' (e.g. Tylecote 1986). Some authors (e.g. Reed *et al.* 2006, Dungworth 2011) have remaining qualms about the lack of evidence for furnace superstructure, but most have now followed the work of Crew (1987, 1989,

1991, 1998) in assuming a now truncated superstructure (shaft) originally overlay these pits and that the lack of evidence in many cases is as a result of truncation (i.e. it is an absence of evidence for the shaft, rather than evidence of absence). The usual model for the operation of these furnaces is that the pits were packed with a combustible organic material prior to the smelt (either grass/cereals or wood) and that late in the smelt (the main reaction of which takes place in the shaft) the slag descending from the growing bloom of iron descends into the pit, creating more space for the bloom to grow, and achieving a better iron-slag separation (cf. Carlin 2008, Illustration 5.2).

No convincing morphological differences in the pre- and post-Roman slagpit furnaces of England have been identified, nor are there yet any archaeometallurgical indicators. The present example might therefore date from either period.

Glossary

Bog Iron Ore: hydrated iron oxide ores formed in superficial sediments (including, but not limited to bogs) through the oxidation of iron-bearing groundwaters.

Cotectic: crystallisation of a liquid to produce two phases at the same time.

Dendrite: a branched crystal form, often associated with rapid growth.

Euhedral: a crystal shape in which the crystal has developed its faces, indicating its growth was unobstructed by previously formed phases.

Fayalite: the iron-rich end member of the olivine group, Fe_2SiO_4 .

Forsterite: the magnesium-rich end member of the olivine group, Mg_2SiO_4 .

Goethite: a hydrated iron III oxide, $\text{FeO}\cdot\text{OH}$.

Gossan: the iron oxide-rich material formed from the superficial oxidation of sulphidic mineral veins

Hematite: an iron III oxide Fe_2O_3

Hercynite: an iron-aluminium member of the spinel group of minerals: FeAl_2O_4

Kaolinite: a hydrous alumina-silicate clay mineral, the major component of china clay, $\text{Al}_2\text{Si}_2\text{O}_5(\text{OH})_4$

Leucite: a potassium-bearing mineral KAlSi_2O_6

Magnetite: an iron oxide member of the spinel group, Fe_3O_4 .

Olivine: a group of silicate minerals of the form $(\text{M}^{2+})_2\text{SiO}_4$ where M can commonly be iron, magnesium, calcium (up to half the M^{2+} ions) or manganese

Slagpit Furnace: a variety of bloomery iron smelting furnace in which much of the slag formed during the smelt drains into a pit below the shaft (rather than being tapped outside the furnace).

Spinel: a mineral group with the general formula $\text{X}^{2+}\text{Y}^{3+}_2\text{O}_4$, which includes, amongst many others, the minerals hercynite and magnetite.

Subhedral: a form of crystal growth which is impeded by some pre-existing phases to permit only some of a crystal's faces to be developed.

Vesicle: a void, usually rounded and formed as a preserved gas bubble in a solidified melt.

Wustite: an iron II oxide FeO

References

- CARLIN, N., 2008 Ironworking and production: an evaluation and assessment of the metallurgical evidence, pp. 87–112, N Carlin, L Clarke and F Walsh *The Archaeology of Life and Death on the Boyne Floodplain: The Linear Landscape of the M4*. Dublin, National Roads Authority, Wordwell.
- CREW, P. 1995. *Bloomery iron smelting, slags and other residues*. Historical Metallurgy Society, Archaeology Datasheet No. 5.
- CREW, P. 1996. *Bloom refining and smithing, slags and other residues*. Historical Metallurgy Society, Archaeology Datasheet No. 6.
- CREW, P. 1987. Bryn y Castell Hillfort – a Late Prehistoric Iron Working settlement in northwest Wales. In: SCOTT, B.G. & CLEERE, H. (eds) *The Crafts of the Blacksmith*. 91-100.
- CREW, P. 1989. Crawcwellt West excavations 1986-1989. A late prehistoric ironworking settlement. *Archaeology in Wales*, **29**, 11-16.
- CREW, P. 1991. The Experimental Production of Prehistoric Bar Iron, *Historical Metallurgy*, **25**, 21-36
- CREW, P. 1998. Excavations at Crawcwellt West, Merioneth, 1990-98: A late prehistoric upland iron-working settlement. *Archaeology in Wales*, **38**, 22-35.
- DINES, H.G. 1956. *The metalliferous mining region of South-West England*. British Geological Survey.
- DUNGWORTH, D. 2010. The possible water-powered bloomery at Goscote (Rushall), Walsall, West Midlands. *Historical Metallurgy*, **44**, 15-20.
- DUNGWORTH, D. 2011. Examination of metalworking debris from the 1939 excavations at Trevelgue Head', in Nowakowski, J and Quinnell, H, *Trevelgue Head, Cornwall - an Iron Age cliffcastle: the story of the 1939 excavations by the late C K Croft Andrew*. Truro: Cornwall County Council.
- FOX, A. 1954. Excavations at Kestor, an early Iron Age settlement near Chagford, Devon. *Transactions of the Devon Association for the advancement of Science*, **86**, 21–62
- HASLAM, J. 1980. A middle Saxon iron smelting site at Ramsbury, Wiltshire. *Medieval Archaeology*, **24**, 1-68.
- MORTON, G.R. & WINGROVE, J. 1969. Constitution of bloomery slags: Part 1: Roman. *Journal of the Iron and Steel Institute*, **207**, 1556-1564
- MORTON, G.R. & WINGROVE, J. 1972. Constitution of bloomery slags: Part II: Medieval. *Journal of the Iron and Steel Institute*, **210**, 478–488.
- PLEINER, R. 2000. *Iron in Archaeology: The European bloomery smelters*, Prague.
- REED, S.J., JULEFF, G. & BAYER, O.J. 2006. Three late Saxon iron-smelting furnaces at Burlescombe, Devon. *Proceedings of the Devon Archaeological Society*, **64**, 71-122.
- THOMAS G.R. & YOUNG, T.P. 1999a. Bloomery furnace mass balance and efficiency. In: POLLARD, A.M. (ed) *Geoarchaeology: exploration, environments, resources*, Geological Society of London, Special Publication, 165, 155-164.
- THOMAS, G.R. & YOUNG, T.P. 1999b. A graphical method to determine furnace efficiency and lining contribution to Romano-British bloomery iron-making slags (Bristol Channel Orefield, UK). In: YOUNG, S.M.M., BUDD, P.D., IXER, R.A. and POLLARD, A.M. (eds). *Metals in Antiquity*, British Archaeological Reports International Serie
- TYLECOTE, R.F. 1986. *The prehistory of metallurgy in the British Isles*. The Institute of Metals. 257pp.
- YOUNG, T.P. 2003a. Evaluation of slag from Tullyallen 6, Co. Louth (00E00944). *GeoArch Report 2003/10*. 2pp. + 2 figs.
- YOUNG, T.P. 2003b. Is the Irish iron-smelting bowl furnace a myth? A discussion of new evidence for Irish bloomery iron making. *GeoArch Report 2003/09*. 4pp.
- YOUNG, T.P. 2005. Evaluation of metallurgical residues from Hartshill Copse (HCB01). *GeoArch Report 2005/06*. 7pp + 2 figs.
- YOUNG, T.P. 2006. Evaluation of archaeometallurgical residues from sites on the N25, Co. Waterford (Woodstown 6, Adamstown 1,2,3). *GeoArch Report 2006/15*. 38pp.
- YOUNG, T.P. 2008. Archaeometallurgical residues from Richard Lander School (RLS04) and Truro College (TCF05). *GeoArch Report 2007/22*. 31pp. & 10 plates
- YOUNG, T.P. 2009. The Iron Slag, p. 121-123, in: P. Manning & H. Quinnell, Excavation and field survey at the Iron Age hillfort of Berry Ball, Crediton Hamlets. *Proceedings of the Devon Archaeological Society*, **67**, 99-132.
- YOUNG, T.P., 2011a. Archaeometallurgical residues from Ned's Garden & Cindermill, Shropshire. *GeoArch Report 2011/10*. 48pp.
- YOUNG, T.P., 2011b. Archaeometallurgical residues from the N7 Castletown to Nenagh scheme, Camlin 3 (E3580), Co. Tipperary. *GeoArch Report 2011/23*. 62 pp.
- YOUNG, T.P. & KEARNS, T. 2011. Evaluation of archaeometallurgical residues from sites D1 and D5, Avon SWW pipeline, Devon. *GeoArch Report 2010/08*. 6pp.

Figure Captions

Figure 1

EDS bulk slag analyses plotted on the CaO-SiO₂-FeO ternary diagram.

Plate A1

Sample AVN21, particle 'A', backscattered electron micrographs.

- a. SOI 1; scale bar 5mm
- b. SOI 2; scale bar 600µm.
- c. SOI 3; scale bar 70 µm.
- d. SOI 4; scale bar 100 µm.
- e. SOI 5; scale bar 60 µm.
- f. SOI 10; scale bar 40µm.
- g. SOI 11; scale bar 300µm.
- h. SOI 12; scale bar 300µm.

Plate A2

Sample AVN21, particle 'A', backscattered electron micrographs.

- a. SOI 13; scale bar 40µm.
- b. SOI 14; scale bar 100µm.
- c. SOI 15; scale bar 40µm.

Plate A3

Sample AVN21, particle 'B', backscattered electron micrographs.

- a. SOI 6; scale bar 5mm.
- b. SOI 7; scale bar 600µm.
- c. SOI 8; scale bar 100µm.
- d. SOI 9; scale bar 60µm.
- e. SOI 16; scale bar 70µm.
- f. SOI 17; scale bar 600µm.
- g. SOI 18; scale bar 600µm.

Plate A4

Sample AVN22, backscattered electron micrographs.

- a. SOI 1; scale bar 1mm.
- b. SOI 2; scale bar 60µm.
- c. SOI 3; scale bar 600µm.
- d. SOI 4; scale bar 70µm.
- e. SOI 5; scale bar 600µm.
- f. SOI 6; scale bar 600µm.

Plate A5

Sample AVN23, backscattered electron micrographs.

- a. SOI 1; scale bar 1mm.
- b. SOI 2; scale bar 300µm.
- c. SOI 3; scale bar 600µm.
- d. SOI 4; scale bar 100µm.
- e. SOI 5; scale bar 70µm.
- f. SOI 6; scale bar 300µm.
- g. SOI 7; scale bar 300µm.

Plate A6

Sample AVN24, backscattered electron micrographs.

- a. SOI 10; scale bar 1mm.
- b. SOI 11; scale bar 100µm.
- c. SOI 12; scale bar 300µm.
- d. SOI 13; scale bar 100µm.
- e. SOI 14; scale bar 600µm.
- f. SOI 15; scale bar 300µm.
- g. SOI 16; scale bar 400µm.
- h. SOI 17; scale bar 600µm.

Table 1. Material sampled from D5

Code	Context	Sample	Weight	Notes
AVN21	1186	13	10g	Two c. 10mm rounded particles, dimpled or lobate spheroids
AVN22	1186	13	22g	Blebbly flow slag, 40x35x14mm, upper surface smooth grey, lower surface with rusty furnace floor accretion
AVN23	1186	13	16g	Flow slag sheet, 45mm x 22mm and 5mm thick, impression of wood on one planar surface, attached rounded blebs on the other
AVN24	1429	21	38g	Block of slag rich in fine charcoal particles and also some denser rounded slag particles, 45x30x35mm.

Table 2: Area EDS analyses of typical areas within the samples. Data recast as normalised weight% oxides, with oxygen calculated by stoichiometry.

Sample	Area	Spectrum	SiO ₂	Al ₂ O ₃	FeO	MnO	MgO	CaO	Na ₂ O	K ₂ O	TiO ₂	P ₂ O ₅
AVN 21 A	SOI 10	#13	22.03	9.53	62.51	1.83	0.39	0.93	0.79	1.76	0.24	b.d.
AVN 21 A	SOI 11	#1	20.46	7.74	66.92	2.02	0.55	0.72	0.58	1.02	b.d.	b.d.
AVN 21 A	SOI 12	#1	9.62	3.84	84.19	1.59	0.48	0.28	b.d.	b.d.	b.d.	b.d.
AVN 21 A	SOI 14	#1	20.30	7.22	68.29	1.92	0.46	0.64	0.44	0.72	b.d.	b.d.
AVN 21 B	SOI 17	#1	24.90	8.07	61.91	2.11	0.41	0.87	1.10	0.63	b.d.	b.d.
AVN 21 B	SOI 17	#2	25.75	7.91	61.08	1.96	0.58	0.81	1.22	0.69	b.d.	b.d.
AVN 21 B	SOI 18	#1	23.29	7.32	65.94	2.09	0.37	0.99	b.d.	b.d.	b.d.	b.d.
AVN 22	SOI 3	#1	17.01	4.80	75.24	1.95	0.60	0.31	b.d.	0.10	b.d.	b.d.
AVN 22	SOI 3	#2	16.64	7.12	73.63	1.80	0.47	0.33	b.d.	b.d.	b.d.	b.d.
AVN 22	SOI 3	#3	17.35	7.07	72.45	1.90	0.32	0.40	b.d.	0.30	0.21	b.d.
AVN 22	SOI 4	#11	15.22	8.86	73.19	1.65	0.44	0.40	b.d.	b.d.	0.24	b.d.
AVN 22	SOI 5	#1	8.12	3.87	86.02	1.51	0.48	b.d.	b.d.	b.d.	b.d.	b.d.
AVN 22	SOI 6	#1	17.85	7.28	71.39	1.96	0.42	0.52	b.d.	0.59	b.d.	b.d.
AVN 23	SOI 3	#2	25.19	8.54	60.79	2.41	0.79	0.84	0.64	0.19	0.30	0.30
AVN 23	SOI 6	#1	26.10	9.53	57.62	2.17	0.52	1.16	0.87	1.74	b.d.	0.30
AVN 23	SOI 7	#1	26.97	10.36	55.63	2.03	0.41	1.42	0.81	2.07	0.29	b.d.
AVN 24	SOI 14	#1	21.97	10.28	60.93	4.59	0.61	1.24	b.d.	0.39	b.d.	b.d.
AVN 24	SOI 14	#2	20.71	10.87	61.70	4.71	0.70	0.77	b.d.	0.20	0.35	b.d.
AVN 24	SOI 15	#1	22.71	8.29	60.93	4.04	0.55	1.22	0.56	1.40	b.d.	0.30
AVN 24	SOI 16	#3	25.50	9.77	55.62	4.16	0.53	1.57	0.93	1.59	0.33	b.d.
AVN 24	SOI 17	#1	19.38	9.04	64.67	4.23	0.55	1.19	b.d.	0.20	0.28	0.47

Table 3. EDS analyses of phases in samples from D5, presented as normalised atomic percentages; analyses arranged by sample and phase. i/s = interstitial, b.d. = below detection

					O	Na	Mg	Al	Si	P	S	Cl	K	Ca	Ti	V	Cr	Mn	Fe	Ba	Ce	W
21	SOI 10	#1	point	wustite	49.53										0.12			0.49	49.86			
21	SOI 10	#12	point	wustite	49.50			0.39	0.20						0.12			0.50	49.29			
21	SOI 13	#6	point	wustite	49.35			0.48										0.56	49.61			
21	SOI 16	#3	point	wustite	48.10			0.17	0.51					0.11	0.11			0.38	50.62			
21	SOI 16	#17	point	wustite (with leucite)	56.23	1.87		5.36	4.30	8.37			0.27		0.13			0.12	23.35			
21	SOI 16	#21	point	wustite (with leucite)	57.74	0.57		7.96	13.28				5.68		0.13			0.10	14.54			
21	SOI 13	#8	point	magnetite lamella	54.23			0.57										0.35	44.84			
21	SOI 10	#2	point	hercynite dendrite	56.44	0.50		23.97	2.70				0.45	0.14	0.15			0.28	15.37			
21	SOI 10	#3	point	hercynite dendrite	56.48	0.32		23.43	3.51				0.57	0.12	0.12			0.30	15.15			
21	SOI 10	#11	point	hercynite dendrite	56.87			23.20	2.88				0.56		0.13			0.35	16.02			
21	SOI 10	#16	point	hercynite on wustite	55.11			18.28	3.55						0.19			0.50	22.38			
21	SOI 10	#17	point	hercynite on wustite	55.44		0.29	11.96	7.69				0.26	0.21				0.68	23.47			
21	SOI 13	#2	point	hercynite	56.70		0.33	23.63	1.27						0.09			0.40	17.57			
21	SOI 13	#3	point	hercynite	56.17		0.33	24.42	0.60						0.10			0.33	18.04			
21	SOI 13	#7	point	hercynite	54.90		0.27	23.41	1.20									0.45	19.76			
21	SOI 15	#6	point	hercynite	55.67			20.98	3.03				0.10	0.09	0.15			0.49	19.49			
21	SOI 15	#7	point	hercynite	55.88	0.00		22.07	2.64					0.07	0.17			0.43	18.75			
21	SOI 15	#12	point	hercynite	56.22			24.13	2.07				0.23		0.19			0.35	16.81			
21	SOI 16	#10	point	hercynite	56.41			25.58	0.19						0.30			0.29	17.16			0.06
21	SOI 16	#11	point	hercynite	55.72			25.31	0.42						0.24			0.38	17.93			
21	SOI 10	#4	point	olivine core	55.99		0.79	0.36	14.43					0.13				1.18	27.11			
21	SOI 10	#5	point	olivine core	56.39		0.99	0.37	14.09					0.10				1.20	26.86			
21	SOI 10	#6	point	olivine middle	56.27		0.94	0.44	14.07					0.13				1.24	26.91			
21	SOI 10	#7	point	olivine margin	56.26		0.69	0.45	14.34				0.13	0.12				1.12	26.89			
21	SOI 10	#8	point	olivine margin	58.00	0.51		2.43	13.63				1.28	0.77				0.87	22.52			
21	SOI 10	#9	point	i/s olivine	57.31			2.84	13.36				0.45	0.36				1.07	24.61			
21	SOI 10	#10	point	i/s olivine	59.24	1.15		4.81	14.62	0.16			2.61	1.07				0.62	15.72			
21	SOI 13	#1	point	olivine	56.56		0.89	0.42	14.18									1.18	26.77			
21	SOI 13	#4	point	olivine	56.17		0.98	0.44	14.21									1.22	26.98			
21	SOI 13	#5	point	olivine	57.32		0.97	0.53	13.80					0.12				1.18	26.08			

					O	Na	Mg	Al	Si	P	S	Cl	K	Ca	Ti	V	Cr	Mn	Fe	Ba	Ce	W
21	SOI 15	#2	point	olivine inner	57.58		0.79	0.75	14.05				0.44	0.26				1.10	25.02			
21	SOI 15	#3	point	olivine	56.55		0.69	0.35	14.04					0.12				1.16	27.09			
21	SOI 15	#4	point	olivine	56.41		0.35	0.47	14.07					0.18				1.20	27.31			
21	SOI 15	#5	point	olivine	56.66		0.38	3.88	11.89				0.16	0.21				0.95	25.87			
21	SOI 15	#9	point	olivine outer	56.70		0.30	0.36	14.29					0.28				1.16	26.90			
21	SOI 15	#10	point	olivine inner	56.58		0.65	0.44	13.99					0.16				1.14	27.04			
21	SOI 15	#11	point	olivine inner	56.76		0.90	0.38	14.10					0.12				1.21	26.55			
21	SOI 15	#13	point	olivine inner	56.41		0.63	0.37	14.30					0.10				1.10	27.09			
21	SOI 15	#14	point	olivine inner	56.51		0.90	0.62	13.90					0.09				1.21	26.77			
21	SOI 16	#1	point	i/s/ olivine	59.39	1.08		2.46	14.37				0.30	1.07	0.09			0.45	20.80			
21	SOI 16	#4	point	olivine outer (with W)	55.28		0.27	0.25	13.99					0.44				1.05	28.72			
21	SOI 16	#5	point	olivine inner	55.75		1.03	0.22	14.65									1.16	27.19			
21	SOI 16	#6	point	olivine inner	55.51		1.11		14.48					0.11				1.27	27.52			
21	SOI 16	#7	point	olivine inner	55.85		1.08	0.28	14.46					0.10				1.25	26.98			
21	SOI 16	#8	point	olivine outer (with W)	56.01		0.54	0.25	14.52					0.16				1.13	27.39			
21	SOI 16	#9	point	olivine outer (with H)	56.53			0.24	14.56					0.47				1.07	27.12			
21	SOI 16	#12	point	olivine outer (with H)	55.90		0.34	0.27	14.59					0.14				1.22	27.55			
21	SOI 16	#13	point	olivine outer (with H)	55.40	0.39		0.59	14.67					0.59				0.95	27.40			
21	SOI 16	#14	point	olivine outer (with H)	56.82			3.00	13.04					0.28	0.07			0.86	25.93			
21	SOI 16	#16	point	i/s olivine	58.07	0.61		1.96	14.45				0.49	0.62				0.77	23.04			
21	SOI 10	#14	point	i/s glass?	58.68	2.65		9.61	15.37	0.22	0.15		4.90	2.25				0.20	5.95			
21	SOI 10	#15	point	i/s glass?	57.29	2.74		10.89	15.49	0.21	0.13		4.98	1.84				0.20	6.23			
21	SOI 10	#18	area	typical interstitial area	58.01	2.59		9.73	15.63	0.23	0.19		4.59	2.00				0.24	6.80			
21	SOI 15	#1	point	i/s glass? with iron	46.00	1.39		9.86	11.76	0.19	0.19		4.64	2.12	0.00			0.40	23.45			
21	SOI 15	#8	point	i/s glass or leucite	57.27	2.42		9.78	15.23	0.22	0.28		4.79	2.11				0.17	7.72			
21	SOI 15	#15	point	i/s glass?	58.26	2.24		9.16	15.45	0.24	0.18		4.48	2.01				0.29	7.68			
21	SOI 16	#2	point	leucite	63.68	2.96		9.68	17.21	0.00			4.86					1.51	0.09			
21	SOI 16	#15	point	leucite	59.41	0.39		10.48	19.73				9.44					0.42	0.13			
21	SOI 16	#18	point	leucite	59.39			10.24	19.68				10.24		0.08			0.38				
21	SOI 16	#19	point	leucite	63.33	4.63		10.22	19.43				1.44		0.11			0.83				
21	SOI 16	#20	point	leucite	63.09	1.23		9.81	17.59				7.65		0.10			0.53				
21	SOI 16	#22	area	area of L-W	59.61	1.54		9.83	15.62				5.66					7.64	0.10			

					O	Na	Mg	Al	Si	P	S	Cl	K	Ca	Ti	V	Cr	Mn	Fe	Ba	Ce	W
22	SOI 4	#2	point	hercynite dendrite	62.24			24.16	1.71	0.13				0.08	0.06			0.25	11.38			
22	SOI 4	#3	point	hercynite dendrite	58.44			25.75	0.75						0.12			0.33	14.61			
22	SOI 4	#9	point	hercynite dendrite	56.95			24.49	1.00						0.08			0.36	17.11			
22	SOI 4	#12	point	hercynite on wustite	56.22			21.16	2.48					0.11	0.18			0.37	19.48			
22	SOI 4	#13	point	hercynite	55.80			24.92	0.65						0.13			0.43	18.08			
22	SOI 4	#15	point	hercynite on wustite	54.69			14.29	4.50					0.12				0.55	25.85			
22	SOI 4	#4	point	olivine inner	56.65		0.92	0.21	14.09					0.14				1.16	26.84			
22	SOI 4	#5	point	olivine inner	56.25		0.86	0.36	14.06					0.11				1.17	27.19			
22	SOI 4	#6	point	olivine outer	56.61		0.50	0.33	14.03					0.14				1.13	27.25			
22	SOI 4	#7	point	olivine outer	53.23			1.26	13.96					0.41				1.26	29.87			
22	SOI 4	#14	point	olivine outer	56.19		0.39	0.24	14.10					0.13				1.21	27.74			
22	SOI 4	#8	point	olivine inner	56.19		0.60	0.44	13.94					0.10				1.21	27.51			
22	SOI 4	#1	point	i/s glass?	63.31			25.32	5.79	0.32	0.09			0.38				0.10	4.67			
22	SOI 4	#10	point	i/s glass?	55.20			19.99	10.72	0.50	0.19			0.65				0.31	12.27			0.16
23	SOI 3	#1	point	hercynite	53.92		0.46	26.72	0.27						0.20			0.40	18.02			
23	SOI 4	#10	point	hercynite	54.39			25.89							0.74			0.25	18.72			
23	SOI 4	#11	point	hercynite core	53.85		0.75	26.88	0.21						0.16		0.16	0.45	17.55			
23	SOI 4	#12	point	hercynite outer	54.26		0.31	26.35	0.18						0.26			0.37	18.27			
23	SOI 4	#14	point	hercynite	54.52			24.16	0.32						1.07			0.35	19.58			
23	SOI 4	#1	point	olivine core (with w)	53.91		1.32	0.36	15.02									1.34	28.04			
23	SOI 4	#2	point	olivine outer (with W)	54.17		0.77	0.19	15.21					0.13				1.32	28.21			
23	SOI 4	#3	point	olivine outer (with H)	54.70			0.30	14.87					0.41				1.11	28.61			
23	SOI 4	#4	point	olivine outer (with H)	54.34		0.56	0.21	14.91					0.19				1.34	28.45			
23	SOI 4	#5	point	olivine	54.21		0.35	0.19	15.04					0.21				1.22	28.78			
23	SOI 4	#6	point	olivine outer (with H)	54.52		0.34	0.24	14.92					0.26				1.26	28.47			
23	SOI 6	#2	point	olivine inner	54.67		1.48	0.26	14.71					0.13				1.49	27.25			
23	SOI 6	#3	point	olivine margin	55.37			0.27	14.70					0.20				1.32	28.13			
23	SOI 6	#4	point	olivine outer (with H)	54.84		1.34	0.26	14.64									1.37	27.55			
23	SOI 6	#5	point	olivine outer	54.75		1.01	0.22	14.69					0.13				1.33	27.88			
23	SOI 6	#6	point	olivine inner	54.52		1.51	0.25	14.92					0.11				1.23	27.48			

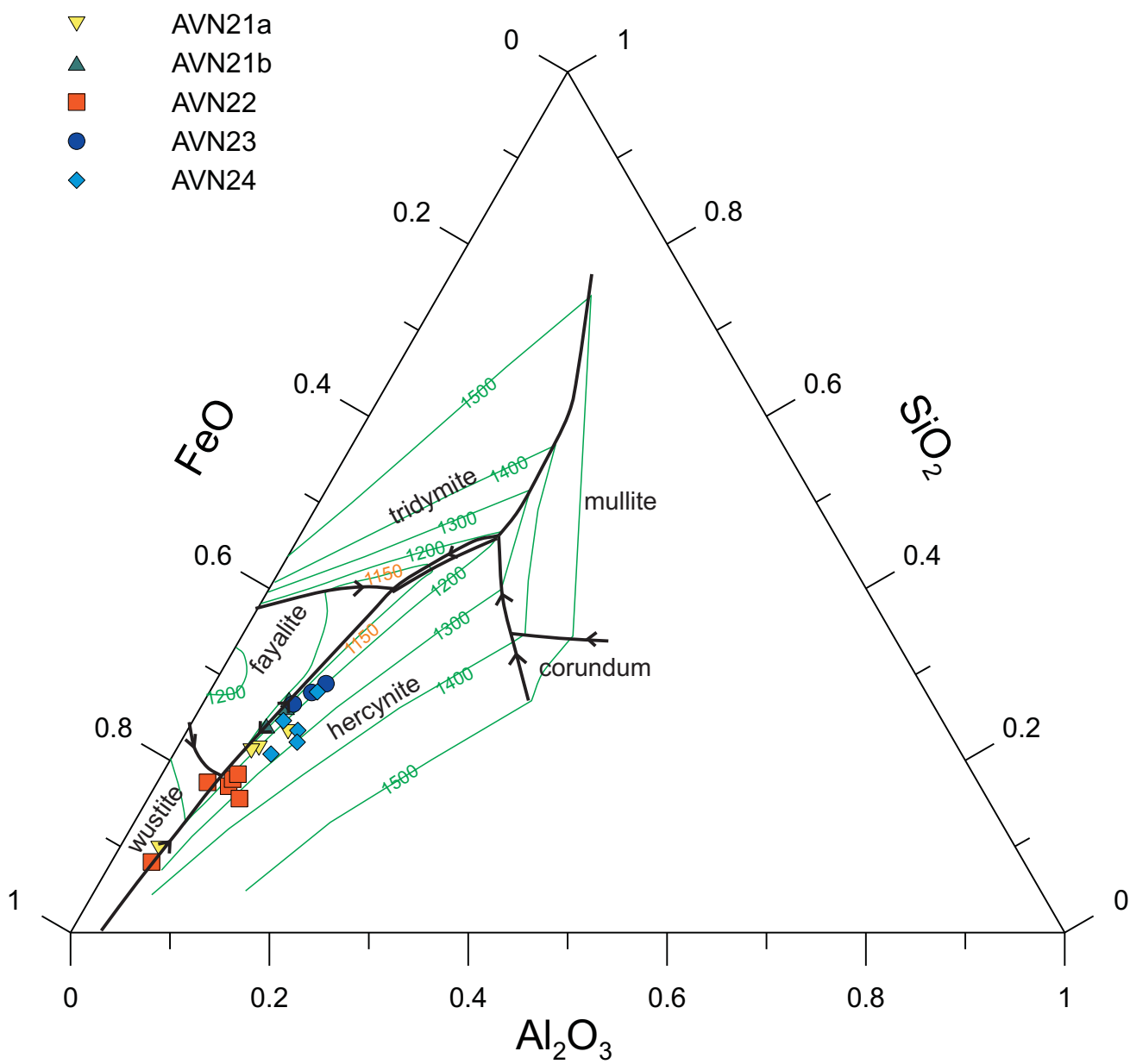
					O	Na	Mg	Al	Si	P	S	Cl	K	Ca	Ti	V	Cr	Mn	Fe	Ba	Ce	W
23	SOI 4	#7	point	leucite	58.42	0.67		10.69	20.37				9.28		0.10				0.47			
23	SOI 5	#3	point	pale i/s	58.38	0.31		10.40	20.18				10.33						0.39			
23	SOI 5	#6	point	pale i/s	58.99	0.49		10.41	19.87				9.64		0.12				0.46			
23	SOI 4	#9	area	W-L	57.89	1.94		9.81	15.87				5.79		0.12				8.59			
23	SOI 4	#8	point	i/s glass?	60.74	4.33		12.20	21.50				0.47	0.17					0.52	0.08		
23	SOI 5	#2	point	dark i/s	60.44	3.99		12.08	22.55				0.46	0.13					0.35			
23	SOI 5	#7	point	dark i/s	60.72	3.62		14.46	19.29	0.35			0.49	0.17					0.90			
23	SOI 5	#1	point	bright i/s phase	54.56	0.51		8.36	10.61				0.10	0.85	0.34			0.60	24.06			
23	SOI 5	#4	point	bright i/s phase	56.60	0.73		2.50	14.24					1.25				0.71	23.98			
23	SOI 5	#8	point	bright i/s phase	57.56	0.84		9.43	4.36	2.78	0.32			3.81	0.21			0.13	20.31			0.24
23	SOI 4	#13	point	apatite mixed	63.71			3.70	4.63	6.19				10.56					11.20			
23	SOI 5	#5	point	apatite mix	61.08			4.28	5.42	5.90				9.79					13.15		0.14	0.24
23	SOI 5	#9	area	apatite mix bulk	62.84			4.95	4.87	5.77				10.34					10.86		0.14	0.25
24	SOI 13	#3	point	wustite in L-W	51.72			0.83	0.23						0.46			0.90	45.86			
24	SOI 13	#4	point	wustite in L-W	55.84			2.03	0.48					0.08	0.55			0.81	40.21			
24	SOI 13	#17	point	wustite in L-W	49.47			0.43	0.23						0.36			1.20	48.31			
24	SOI 13	#7	point	hercynite margin	56.82	0.00	0.00	24.83	0.12						0.42			0.72	17.09			
24	SOI 13	#8	point	hercynite inner	56.08		0.32	25.16	0.20						0.31			0.86	17.07			
24	SOI 13	#9	point	hercynite inner	55.88		0.53	26.04	0.18						0.19			0.81	16.36			
24	SOI 13	#10	point	hercynite inner	55.96		0.76	25.32	0.21						0.20	0.09		0.85	16.59			
24	SOI 13	#14	point	hercynite inner	55.55		0.52	25.21	0.23						0.28			0.90	17.31			
24	SOI 13	#11	point	olivine	56.24		1.34	0.23	14.28					0.18				2.92	24.82			
24	SOI 13	#12	point	olivine inner	56.18		0.40	0.21	14.31					0.32				2.85	25.73			
24	SOI 13	#13	point	olivine	56.21		0.16	0.17	14.47					0.98				2.49	25.53			
24	SOI 13	#5	point	leucite in L-W	31.18			16.80	7.89	0.23		0.12		0.16	0.57			0.91	42.12			

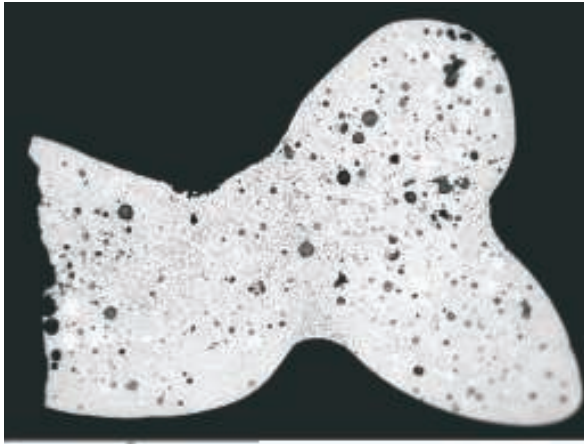
					O	Na	Mg	Al	Si	P	S	Cl	K	Ca	Ti	V	Cr	Mn	Fe	Ba	Ce	W
24	SOI 13	#6	point	leucite in L-W	49.10	0.00		23.80	14.36	0.62	0.46	1.52		0.88					9.26			
24	SOI 16	#2	area	L-W	54.74	0.66		8.20	14.71				6.63		0.14			0.29	14.63			
24	SOI 13	#15	point	weathered area	65.19			2.19	4.15	0.16	0.08		0.09	0.09					28.06			
24	SOI 13	#2	point	outer needle zone	52.88			8.50	12.18	0.87	0.77			6.43	0.23			1.16	16.98			
24	SOI 13	#16	point	bright in needle zone	56.40			9.73	6.64	0.47	0.59			0.62	0.39			0.49	24.67			
24	SOI 16	#1	area	fine i/s	60.06	2.73		7.02	13.19	0.55	0.41		1.04	4.51	0.22			0.51	9.74			
24	SOI 13	#1	point	oxide crust	67.35			1.47	2.57		0.32	0.55						0.21	27.54			

Table 4. Analyses of comparative slags and ores mentioned in the text.

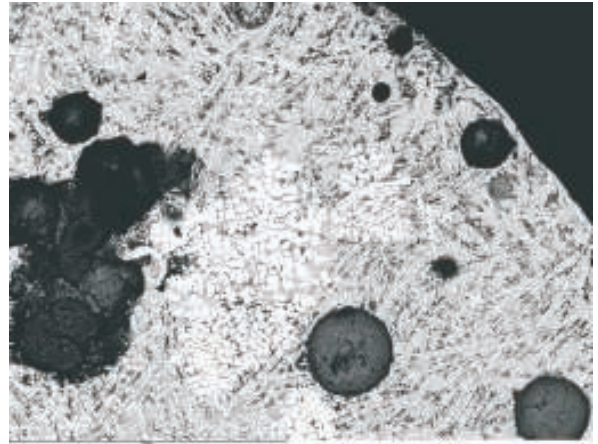
		SiO ₂	Al ₂ O ₃	Fe ₂ O ₃	FeO	MnO	MgO	CaO	Na ₂ O	K ₂ O	TiO ₂	P ₂ O ₅	SO ₃	LOI (observed)	LOI (Fe as Fe ^{II})
Richard Lander School Truro															
RLS-1	stalagmitic flow	21.47	4.16	68.62	61.76	3.41	0.55	1.07	0.27	0.81	0.47	0.99	n.d.	-4.96	1.90
RLS-2a	burr?	17.72	3.85	74.58	67.12	3.41	0.47	0.57	0.28	0.50	0.34	0.99	n.d.	-4.81	2.65
RLS-3	dense slag with charcoal moulds	14.35	2.95	76.66	68.99	3.01	0.46	0.52	0.25	0.25	0.41	0.74	n.d.	-5.26	2.41
TCF-1	slag prill	2.95	0.88	98.36	88.52	1.60	0.17	0.27	0.19	0.18	0.08	0.23	n.d.	-8.05	1.79
RLS-5	ore	2.58	0.41	81.63	73.46	1.09	0.08	0.10	0.18	0.04	0.02	0.99	n.d.	11.81	19.97
RLS-6	ore	3.41	0.26	81.09	72.98	1.35	0.08	0.10	0.21	0.04	0.01	1.07	n.d.	11.91	20.02
Shaugh Prior mine															
Shaugh	Ore analysis, Dines 1956, p.686	5.33	1.1	77.00	67.37	tr	0.25	0.20	n.d.	n.d.	n.d.	1.85			
Kestor (P. Crew samples)															
KES1	Smelting slag: Author's unpub. data	19.92	7.19	67.03	60.32	0.08	0.58	0.28	0.05	0.46	0.15	0.10	0.09	-4.64	2.06
KES2	Hematite ore: Author's unpub. data	0.55	0.20	95.19	85.67	1.43	0.04	<0.004	<0.009	0.02	0.03	0.08	0.06	0.04	9.56
KES3	Hematite/Kaolinite: Author's unpub. data	18.27	14.34	61.65	55.49	0.03	0.47	<0.004	0.13	0.95	0.03	0.05	0.07	1.53	7.70

Figure 1

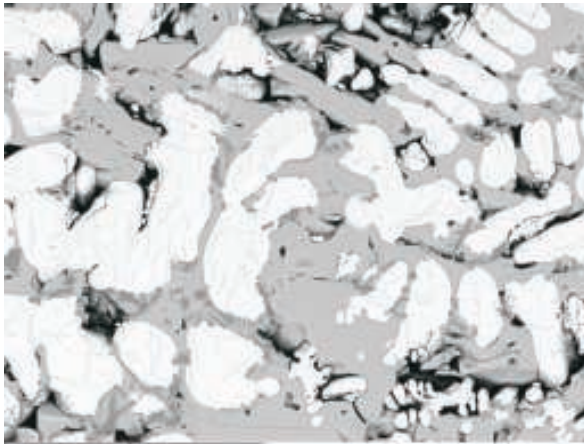




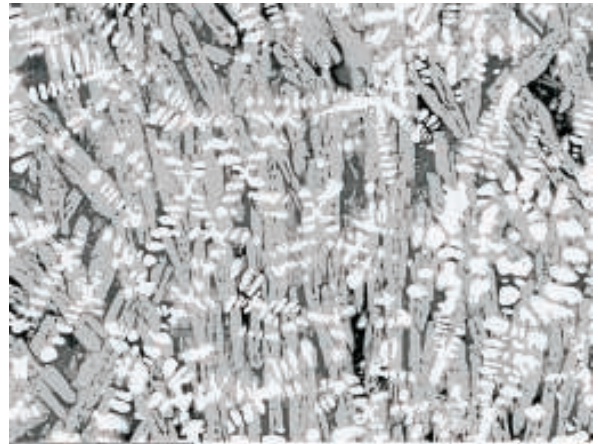
a



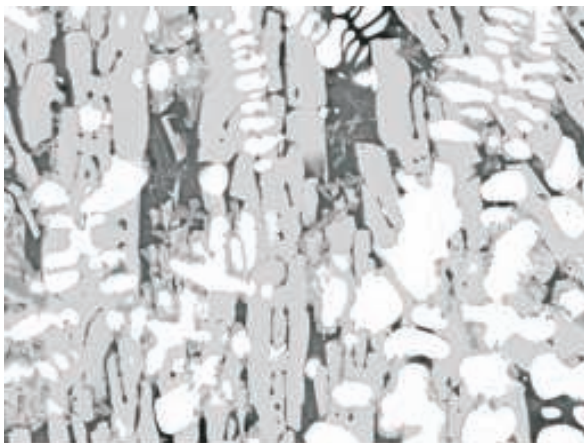
b



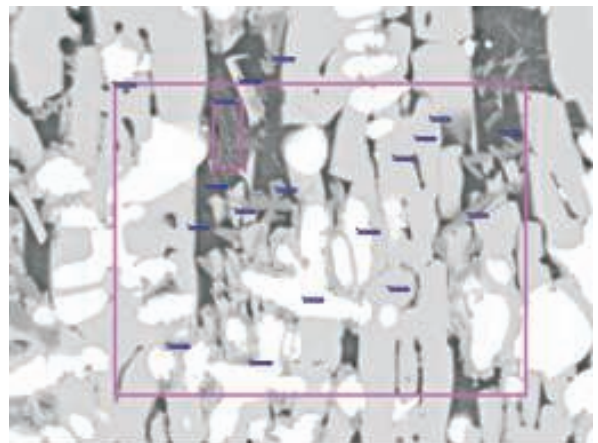
c



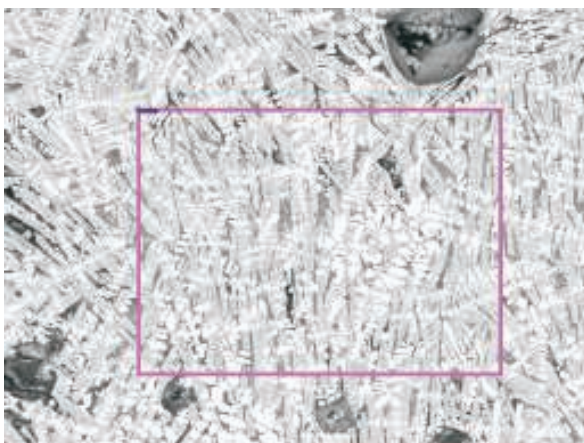
d



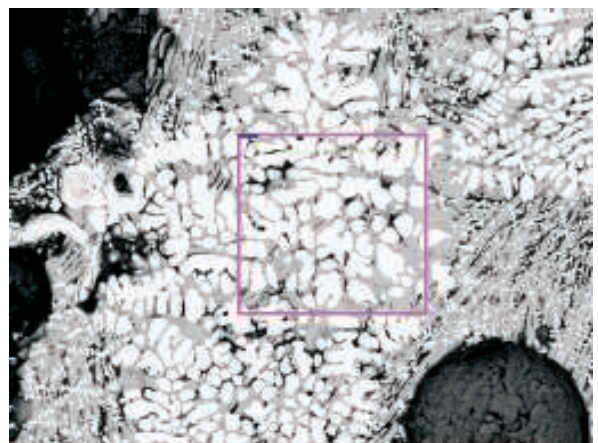
e



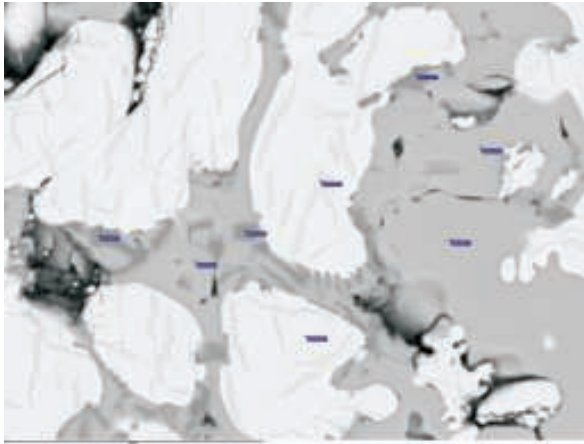
f



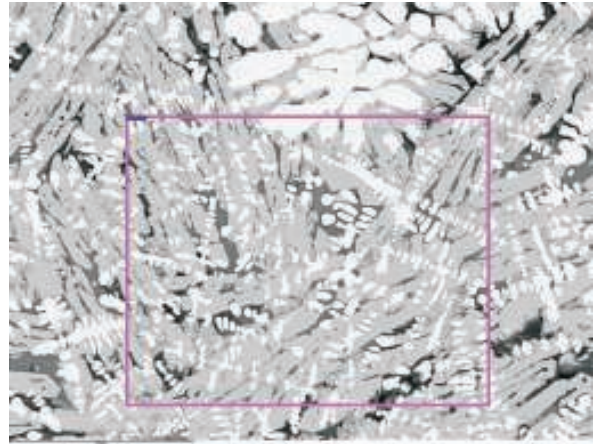
g



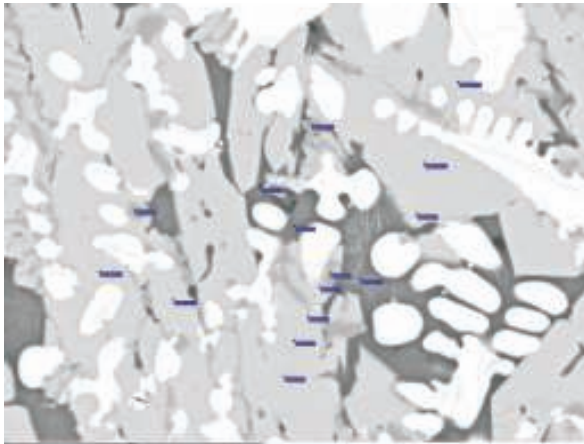
h



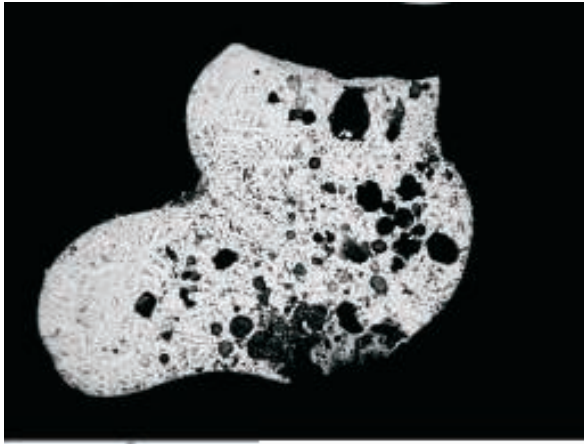
a



b



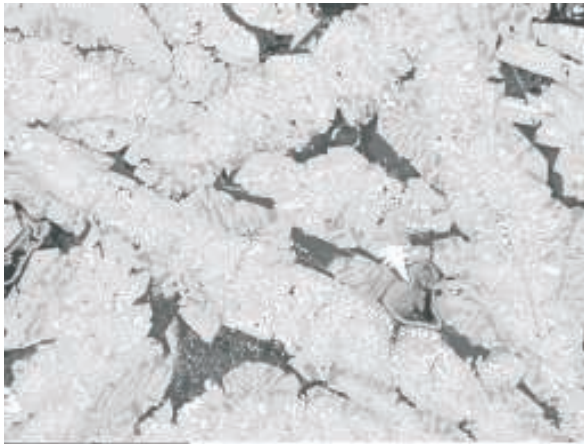
c



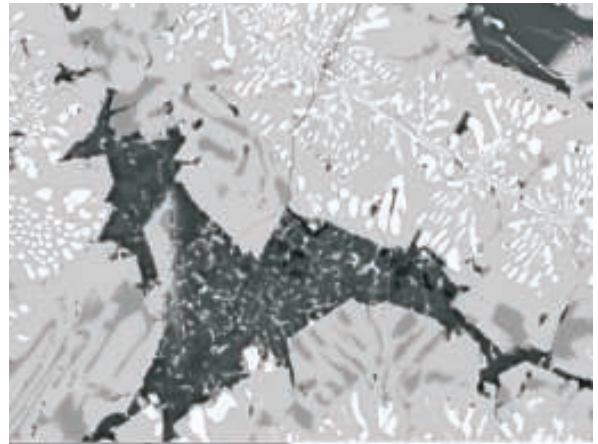
a



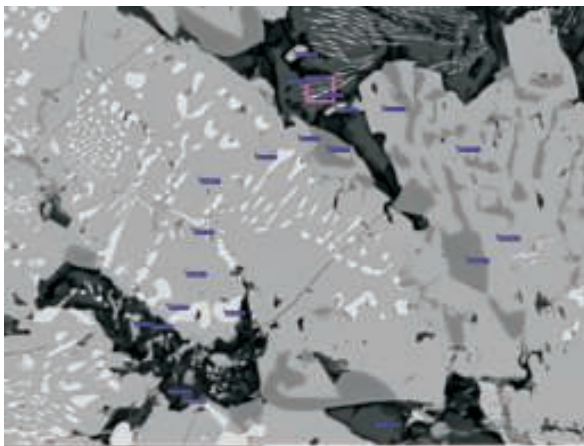
b



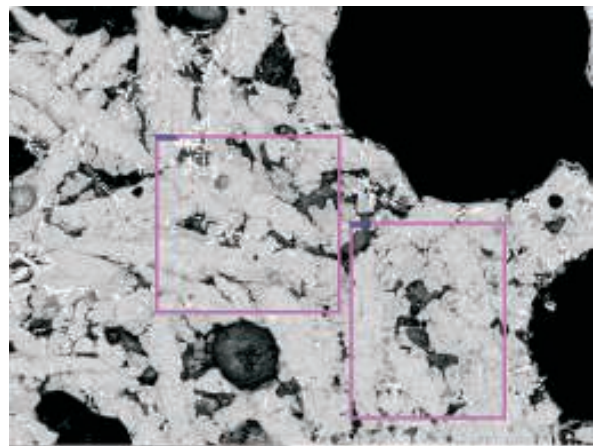
c



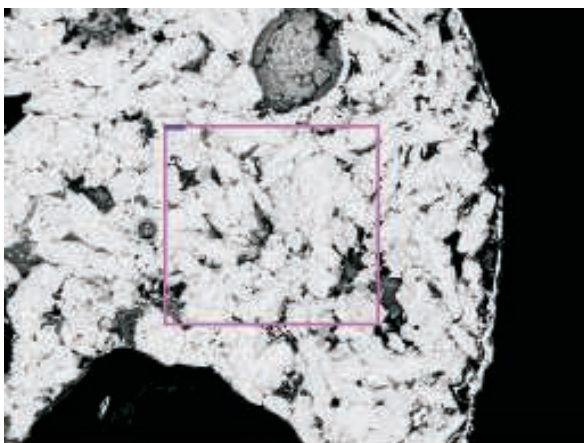
d



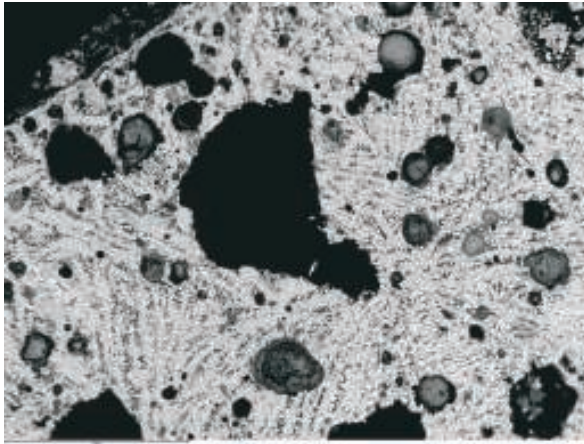
e



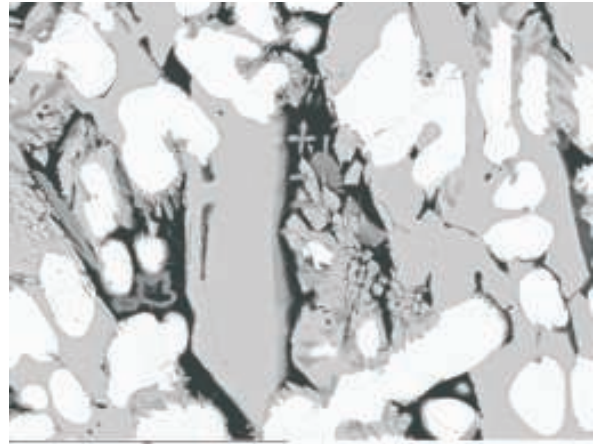
f



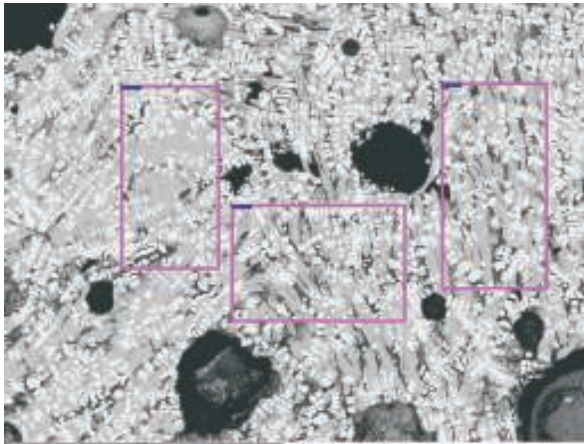
g



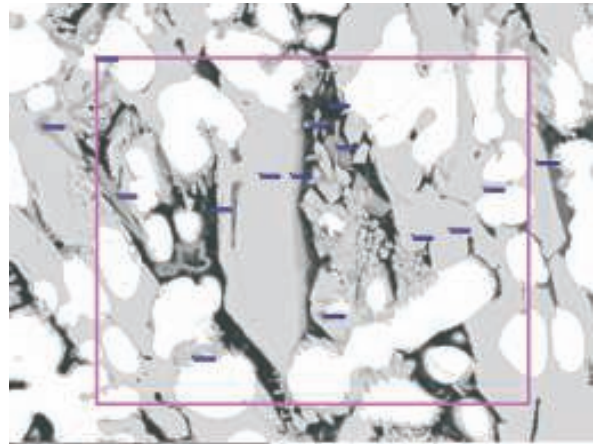
a



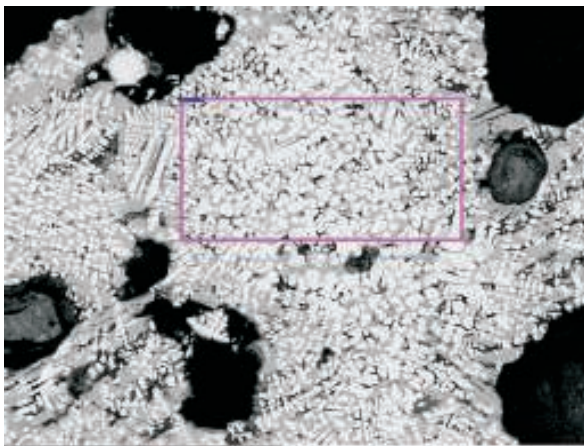
b



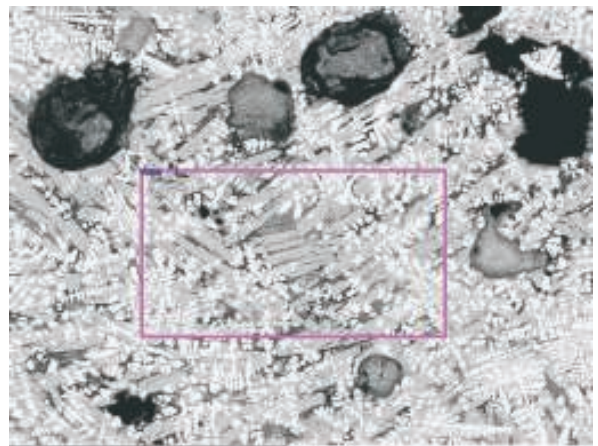
c



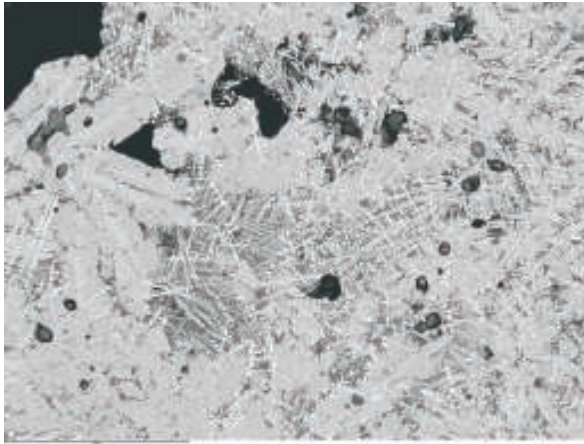
d



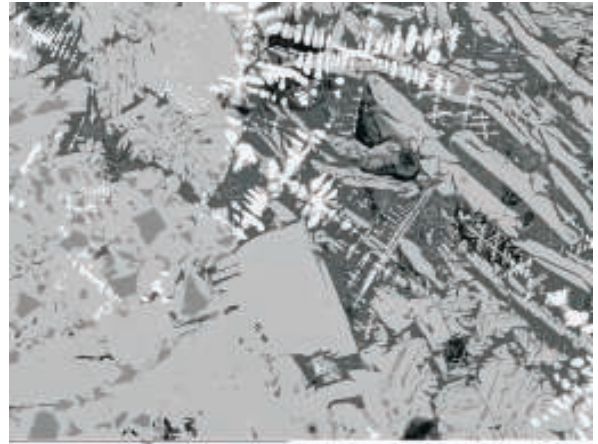
e



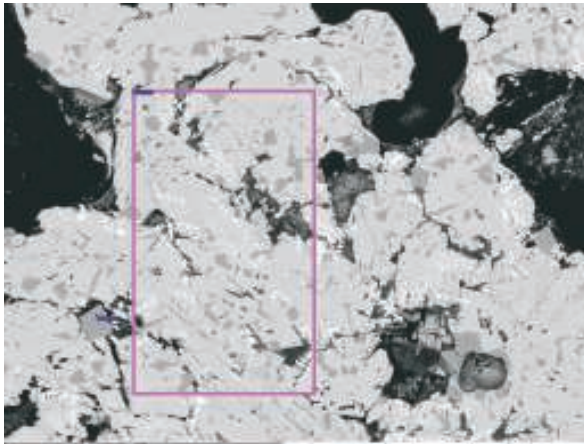
f



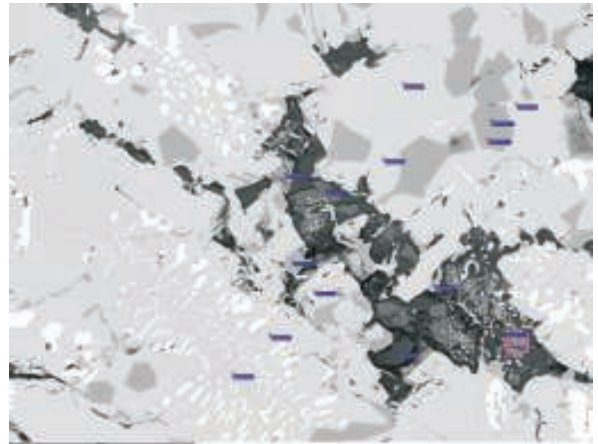
a



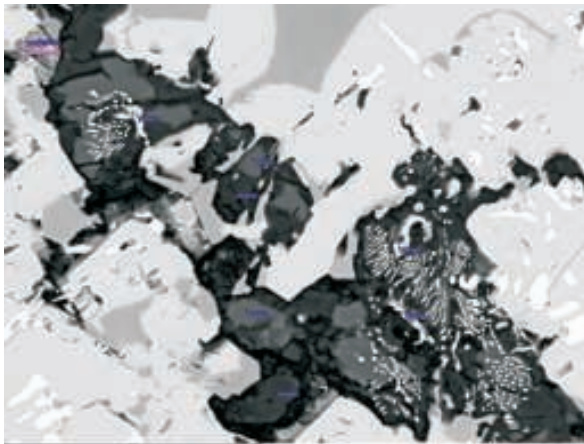
b



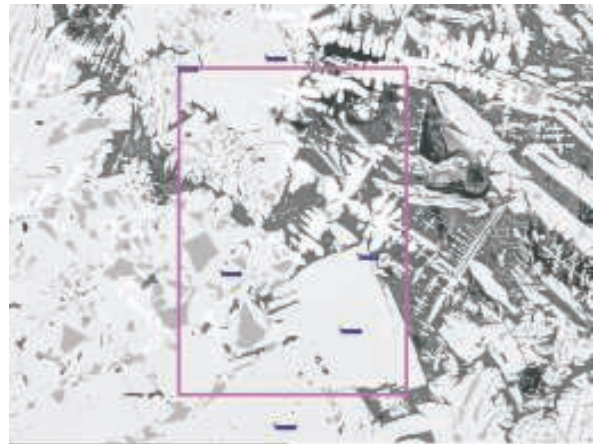
c



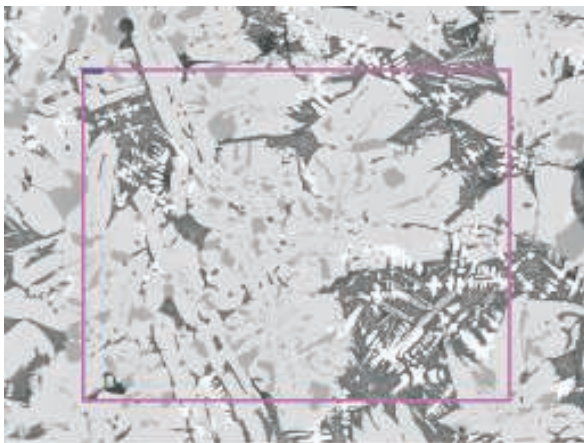
d



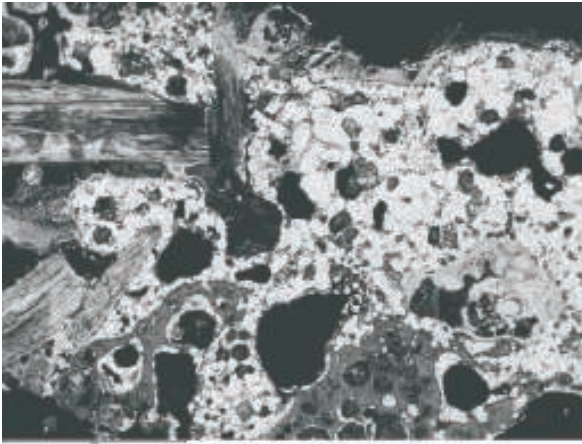
e



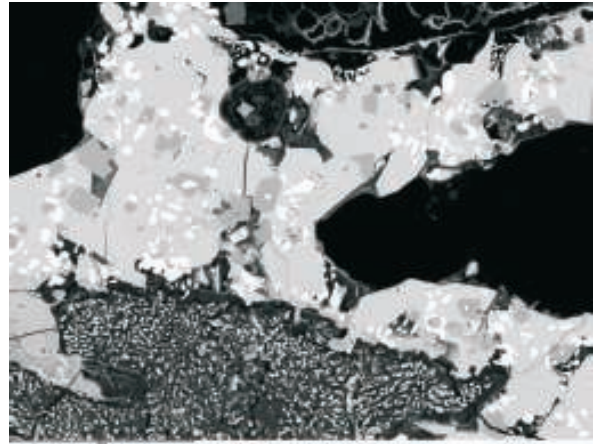
f



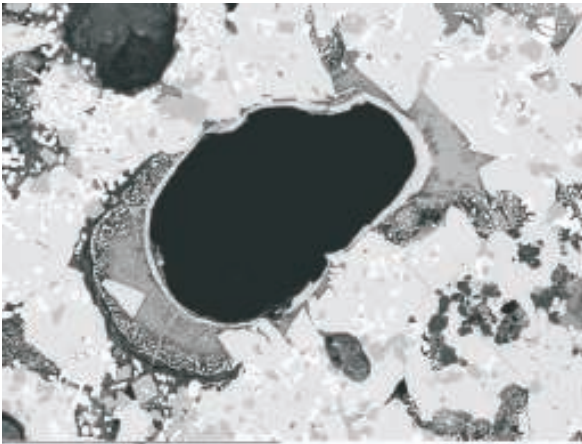
g



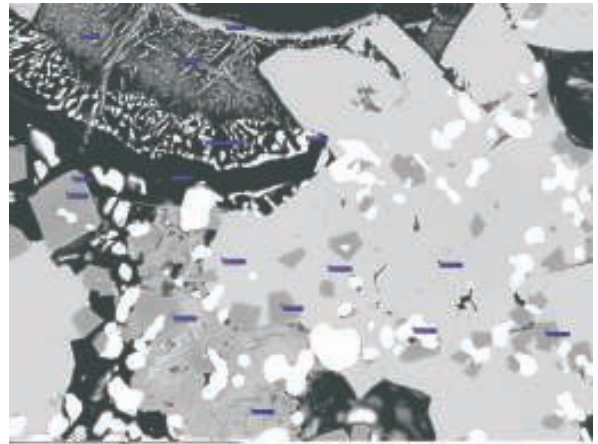
a



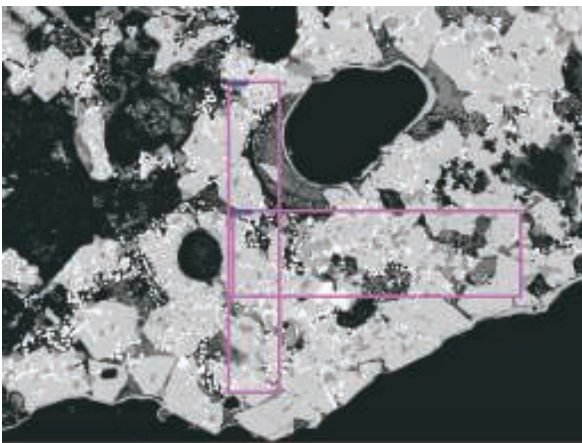
b



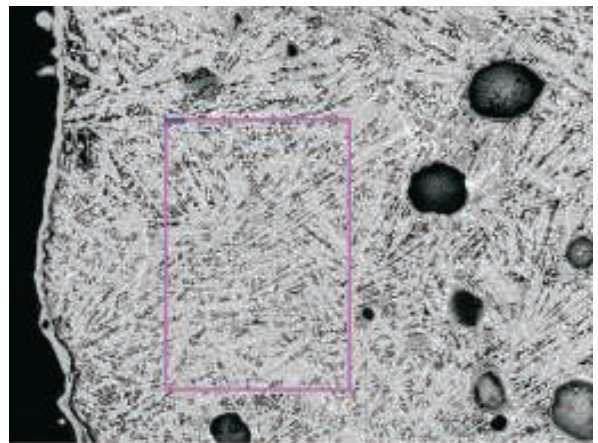
c



d



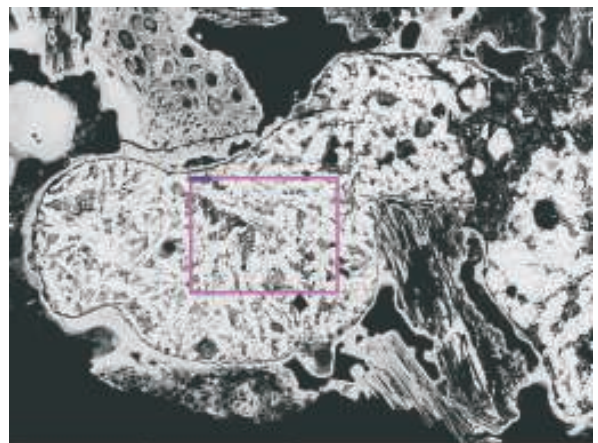
e



f



g



h

GeoArch



geoarchaeological, archaeometallurgical & geophysical investigations

Unit 6,
Western Industrial Estate,
Caerphilly,
CF83 1BQ

<i>Office:</i>	029 20881431
<i>Mobile:</i>	07802 413704
<i>Fax:</i>	08700 547366
<i>E-Mail:</i>	Tim.Young@GeoArch.co.uk
<i>Web:</i>	www.GeoArch.co.uk